

# Escape probability of a photon near the horizon of Kerr-Sen black hole

Ming Zhang<sup>1,\*</sup> and Jie Jiang<sup>2,1,†</sup>

<sup>1</sup>*College of Physics and Communication Electronics,  
Jiangxi Normal University, Nanchang 330022, China*

<sup>2</sup>*Department of Physics, Beijing Normal University, Beijing 100875, China*

The escape probability of a photon emitted from a source static in a locally nonrotating frame is studied. We find that the escape probability of the photon is nonzero in the event horizon limit for the extreme Kerr-Sen black hole. In contrast, the probability becomes vanishing in the horizon limit for the nonextreme Kerr-Sen black hole.

## I. INTRODUCTION

In a recent work [1], Kota Ogasawara et.al. studied the escape probability of a photon emitted from a light source that is at rest in a locally nonrotating frame (LNRF) near the event horizon of the Kerr-Newman black hole. Based on the assumption that all photons are emitted isotropically, they found that the escape probability of a photon emitted from an extreme Kerr-Newman black hole is nonzero in the condition that  $a > 1/2$  with  $a$  the spin per unit mass of the black hole. Specifically, it was obtained that the escape probability becomes a maximum value approximated to 30% if  $a = 1$ . In other conditions, i.e.,  $0 \leq a \leq 1/2$  and the Kerr-Newman black hole is nonextreme, the escape probability of the photon in the horizon limit is zero. According to the work, if the Carter constant is zero, the result on the escape probability of a photon emitted isotropically but confined in the equatorial plane of a Kerr black hole in Ref. [2] can be reproduced.

Recently, the Event Horizon Telescope collaboration released their observation of the shadow of the supermassive black hole candidate in the center of the giant elliptical galaxy M87 [3–8]. The emission ring of the black hole was restored via different calibration and imaging schemes and the observed event-horizon-scale image was shown to be consistent with prospects for a Kerr black hole shadow [3]. The brightness of the transparent emission region which reveals a dark shadow is an important issue in the observation of the black hole shadow. To reconstruct the brightness distribution of the source, signals recorded individually at each station of the very long baseline interferometry require a common time reference attained by local atomic clocks which are paired with the Global Positioning System to assure synchronization [5]. The reconstructed image is characterized by a bright ring whose diameter is  $40 \mu\text{as}$  and an azimuthally asymmetric brightness with interior brightness depressions [6]. The peaked distribution radial brightness profile declines gradually toward the center and the contrast of the brightness at the center compared to the rim was used to confirm the size and width of the cres-

cent shadow [8]. The brightness of the black hole shadow is closely related to the escape probability of the photons [9].

In the region near the black hole, especially the ergosphere between the stationary limit and the event horizon of a rotating black hole, there are typical high-energy events by which some of the energy of the black hole can be extracted and taken away. Penrose suggested a process that a particle dropping into the ergosphere splits into two particles, with one swallowed by the black hole and the other goes back to infinity [10]. Besides the particle disintegration, there are two-particle collision editions, whose energy extraction efficiencies are substantially increased, see Refs. [11–16] for recent instances. To a certain extent, the observability of these high-energy events depends on the escape probability of the massive or massless particles from the region near the black hole [1].

Besides, the first gravitational waves signal from a binary neutron star (designated GW170817) merger was observed to be accompanied by a short gamma-ray burst (designated GRB 170817A) [17], after the first direct detection of gravitational waves and the first observation of a binary stellar-mass black hole merger by the Laser Interferometer Gravitational-Wave Observatory (LIGO) and Virgo [18]. A bright optical transient (identified as AT 2017gfo), X-ray and radio emission were also discovered across the electromagnetic spectrum [17]. This renders that the study of the emission rate, or escape probability, of the electromagnetic waves from a massive compact object like a neutron star or a black hole benefits the multi-messenger observations of the massive merger.

Recently, in [19], we explored the escape probabilities for both massless photons and massive particles being at rest in a locally non-rotating frame (LNRF) from the Kerr-Sen black hole [20]. The particle source was put on the equatorial plane and we assumed that the emitted particles are confined in the equatorial plane. One of our findings is that the escape probabilities of massless photons and massive particles share qualitatively similar properties. In this paper, as a generalization of the work, we will consider that the photons escape isotropically from an equatorial source and are not confined in the equatorial plane in the well-known Kerr-Sen black hole background. Different to the results on the escaping properties of photons in the Kerr-Newman background

\* mingzhang@jxnu.edu.cn

† Corresponding author, jiejiang@mail.bnu.edu.cn

in Ref. [1], as to be seen in what follows, ours here show that all the extreme Kerr-Sen black holes own nonzero photon escape probabilities in the horizon limit. In section II, we will define the emission angles of the photons in the Kerr-Sen spacetime. In section III, we will get the escape cones and evaluate the escape probabilities for the photons in the extreme/nonextreme Kerr-Sen black hole background. The last section will be devoted to our remarks.

## II. EMISSION ANGLES OF PHOTONS IN THE KERR-SEN SPACETIME

The Kerr-Sen line element in the low-energy effective field theory for heterotic string theory can be written in the Boyer-Lindquist coordinates as [20]

$$\begin{aligned} ds^2 &= -\frac{\Delta\rho_c^2}{\Xi} dt^2 + \frac{\rho_c^2}{\Delta} dr^2 + \rho_c^2 d\theta^2 + \frac{\Xi \sin^2 \theta}{\rho_c^2} (d\phi - \omega dt)^2 \\ &= -\frac{\Delta - a^2 \sin^2 \theta}{\Sigma} dt^2 + \frac{\Sigma}{\Delta} dr^2 + \Sigma d\theta^2 \\ &\quad + \frac{\Xi \sin^2(\theta)}{\Sigma} d\phi^2 - \frac{4Mr a \sin^2 \theta}{\Sigma} dt d\phi, \end{aligned} \quad (1)$$

where

$$\begin{aligned} \rho^2 &= r^2 + a^2 \cos^2 \theta, & \rho_c^2 &= \rho^2 + 2cr = \Sigma, \\ \delta &= r^2 + a^2 + 2cr, & \Delta &= \delta - 2Mr, \\ \Xi &= \delta^2 - \Delta a^2 \sin^2 \theta, & \omega &= 2Mar/\Xi, \\ c &= Q^2/(2M), & a &= J/M, \end{aligned}$$

with  $M, Q, J, c$  are mass,  $U(1)$  charge, angular momentum, and twist parameter of the black hole, respectively. The Kerr geometry can be recovered once we set  $c = 0$ .  $\Delta = 0$  yields the Cauchy horizon and the event horizon of the black hole as

$$r_{\text{I}} = M - c - \sqrt{(M - c)^2 - a^2}, \quad (2)$$

$$r_{\text{H}} = M - c + \sqrt{(M - c)^2 - a^2}. \quad (3)$$

To ensure the regularity of the horizons and avoid the occurrence of naked singularity, we must keep

$$0 \leq a \leq a + c \leq M. \quad (4)$$

The black hole becomes extreme if  $a + c = M$ .

Using the Hamilton-Jacobi method or solving the geodesic equation, one can obtain the four-momentum of a photon on geodesic orbit expressed in terms of the first-order differential system as

$$\Sigma p^t = \frac{\delta}{\Delta} (e\delta - al) - a(ae \sin^2 \theta - l), \quad (5a)$$

$$\Sigma p^r = \sigma_r \sqrt{\bar{\mathcal{R}}(r)}, \quad (5b)$$

$$\Sigma p^\theta = \sigma_\theta \sqrt{\bar{\Theta}(\theta)}, \quad (5c)$$

$$\Sigma p^\phi = \frac{a}{\Delta} (e\delta - al) - \csc^2 \theta (ae \sin^2 \theta - l), \quad (5d)$$

where

$$\begin{aligned} \bar{\mathcal{R}}(r) &= (E\delta - aL)^2 - \Delta [\mathcal{Q} + (L - aE)^2], \\ \bar{\Theta}(\theta) &= \mathcal{Q} - (L^2 \csc^2 \theta - a^2 E^2) \cos^2 \theta \end{aligned}$$

are the radial effective potential and the longitude angular effective potential, which, after introducing dimensionless parameters

$$b = \frac{l}{e}, \quad q = \frac{\mathcal{Q}}{e^2}, \quad (6)$$

can be rewritten as

$$\mathcal{R}(r) \equiv \frac{\bar{\mathcal{R}}(r)}{e^2} = (ab - \delta)^2 - \Delta [q + (b - a)^2], \quad (7)$$

$$\Theta(\theta) \equiv \frac{\bar{\Theta}(\theta)}{e^2} = q - (b^2 \csc^2 \theta - a^2) \cos^2 \theta. \quad (8)$$

$E, L, \mathcal{Q}$  are conserved energy, conserved angular momentum parallel to the black hole symmetry axis and Carter constant [21] corresponding to the Killing vectors  $\partial_t, \partial_\phi$  and the Killing-Yano tensor field, respectively.  $\sigma_r, \sigma_\theta = \pm 1$  determine the direction of the photon trajectory and they are independent of each other. The four-momentum of the photon is defined by  $p^a = (\partial/\partial\lambda)^a$  with  $\lambda$  the affine parameter related with the proper time  $\tau$  of the photon with rest mass  $\mu$  by  $\lambda = \tau/\mu$ .

Rather than describing physics in the inconvenient Boyer-Lindquist coordinates for the Kerr-Sen metric (1), we would like to introduce the orthonormal tetrad

$$e_\mu^{(t)} = \left( \sqrt{\frac{\Delta\Sigma}{\Xi}}, 0, 0, 0 \right), \quad (9a)$$

$$e_\mu^{(r)} = \left( 0, \sqrt{\frac{\Sigma}{\Delta}}, 0, 0 \right), \quad (9b)$$

$$e_\mu^{(\theta)} = (0, 0, \sqrt{\Sigma}, 0), \quad (9c)$$

$$e_\mu^{(\varphi)} = \left( -\frac{2aMr \sin \theta}{\sqrt{\Xi\Sigma}}, 0, 0, \sin \theta \sqrt{\frac{\Xi}{\Sigma}} \right), \quad (9d)$$

carried by an observer rotating with the black hole, i.e., an LNRF [22], so that we can use relations

$$e^{(a)} = e_\mu^{(a)} dx^\mu, \quad (10)$$

$$e_{(a)} = e^\mu_{(a)} \frac{\partial}{\partial x^\mu} \quad (11)$$

to transform the basis vectors back and forth between Boyer-Lindquist coordinate frame and the LNRF frame.

The physically measured LNRF components of the photon's four-momentum can be got by

$$p^{(a)} = p^\mu e_\mu^{(a)}, \quad (12)$$

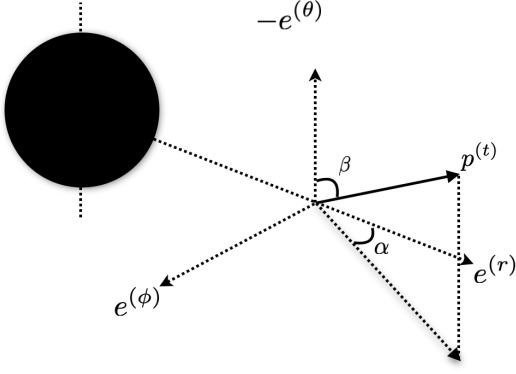


FIG. 1. Projection of the momentum  $p^{(t)}$  in the observer's LNRF for a photon. We choose  $e^{(\theta)}$  as the southward direction.  $\alpha$  is positive in the direction  $e^{(\phi)}$ .

which gives

$$p^{(t)} = \sqrt{\frac{\Delta}{\Xi\Sigma}} \left[ \frac{\delta(\delta e - a l)}{\Delta} + a(l - a e \sin^2 \theta) \right], \quad (13a)$$

$$p^{(r)} = \sigma_r \sqrt{\frac{R}{\Delta\Sigma}}, \quad (13b)$$

$$p^{(\theta)} = \sigma_s \sqrt{\frac{\Theta}{\Sigma}}, \quad (13c)$$

$$p^{(\phi)} = \sin \theta \left[ \frac{2aMr (a^2 \Delta e \sin^2 \theta + a l (\delta - \Delta) - \delta^2 e)}{\Delta \Sigma \sqrt{\Xi \Sigma}} + \frac{(\Delta l \csc^2 \theta - a(al + e(\Delta - \delta)))}{\Delta \Sigma \sqrt{\Sigma/\Xi}} \right]. \quad (13e)$$

Considering a light source staying at rest with a radial position  $r = r_*$  on the equatorial plane of the Kerr-Sen black hole, the emission angles  $(\alpha, \beta)$  of a photon concerning the LNRF can be defined by

$$p^{(r)} = p^{(t)} \cos \alpha \sin \beta, \quad (14a)$$

$$p^{(\theta)} = -p^{(t)} \cos \beta, \quad (14b)$$

$$p^{(\phi)} = p^{(t)} \sin \alpha \sin \beta, \quad (14c)$$

where we have used the relation  $p^{(a)} p_{(a)} = 0$  for the massless photon and we have  $p^{(t)} > 0$  due to the forward-in-time condition. As shown in Fig. 1, the angular coordinate  $\alpha$  is the angle between  $e^{(r)}$  and the projection of  $p^{(t)}$  on the  $e^{(r)} - e^{(\phi)}$  plane, the angular coordinate  $\beta$  is the angle between  $-e^{(\theta)}$  and  $p^{(t)}$ . The domains of  $\alpha, \beta$  are  $[-\pi, \pi]$  and  $[0, \pi]$ , respectively. Starting from this definition, the emission angles can be solved as

$$\sin \alpha = \frac{p^{(\phi)}}{\sqrt{(p^{(r)})^2 + (p^{(\phi)})^2}}, \quad (15a)$$

$$\tan \alpha = \frac{p^{(\phi)}}{p^{(r)}}, \quad (15b)$$

and

$$\sin \beta = \frac{\sqrt{(p^{(r)})^2 + (p^{(\phi)})^2}}{p^{(t)}}, \quad (16a)$$

$$\cos \beta = \frac{p^{(\theta)}}{p^{(t)}}, \quad (16b)$$

which show that the emission angles are associated with some key parameters as

$$\alpha = \alpha(\sigma_r, b, q, r_*), \quad (17)$$

$$\beta = \beta(\sigma_\theta, b, q, r_*). \quad (18)$$

The range of the emission angles can be appointed as

$$-\pi \leq \alpha(\sigma_r = -1, b \leq 0, q, r_*) \leq -\frac{\pi}{2}, \quad (19a)$$

$$\frac{\pi}{2} \leq \alpha(\sigma_r = -1, b \geq 0, q, r_*) \leq \pi, \quad (19b)$$

$$-\frac{\pi}{2} \leq \alpha(\sigma_r = 1, b \leq 0, q, r_*) \leq 0, \quad (19c)$$

$$0 \leq \alpha(\sigma_r = 1, b \geq 0, q, r_*) \leq \frac{\pi}{2}, \quad (19d)$$

and

$$0 \leq \beta(\sigma_\theta = -1, b, q, r_*) \leq \frac{\pi}{2}, \quad (20a)$$

$$\frac{\pi}{2} \leq \beta(\sigma_\theta = 1, b, q, r_*) \leq \pi. \quad (20b)$$

Note that  $\alpha = \pi$  is equivalent to  $\alpha = -\pi$  and both of them correspond to  $b = 0$ . The photon moves on the equatorial plane for  $q = 0$ .

### III. ESCAPE CONES AND ESCAPE PROBABILITIES OF PHOTONS ESCAPING TO INFINITY

To facilitate our reader, we here will use most of our denotations as those in Ref. [1]. We set  $M = 1$ . As the light source we choose is located on the equatorial plane of the Kerr-Sen black hole, we have  $q \geq 0$  according to Eq. (8). By solving  $\mathcal{R} = 0$ , the radial turning points of the photon can be obtained as

$$b = b_1(r) \quad (21)$$

$$= \frac{\sqrt{a^4 \Delta - 2a^2 \delta \Delta + a^2 \Delta q + \delta^2 \Delta - \Delta^2 q - 2ar}}{\Delta - a^2}, \quad (22)$$

and

$$b = b_2(r) \quad (23)$$

$$= \frac{-\sqrt{a^4 \Delta - 2a^2 \delta \Delta + a^2 \Delta q + \delta^2 \Delta - \Delta^2 q - 2ar}}{\Delta - a^2}. \quad (24)$$

$b_2$  diverges at  $r_{b_2} = \sqrt{c^2 - 2c - a^2 + 1} - c + 1$ . To make  $R \geq 0$ , we should have

$$b \leq b_1 \quad \text{for} \quad r_H \leq r < r_{b_2}, \quad (25)$$

$$b_2 \leq b \leq b_1 \quad \text{for } r > r_{b_2}. \quad (26)$$

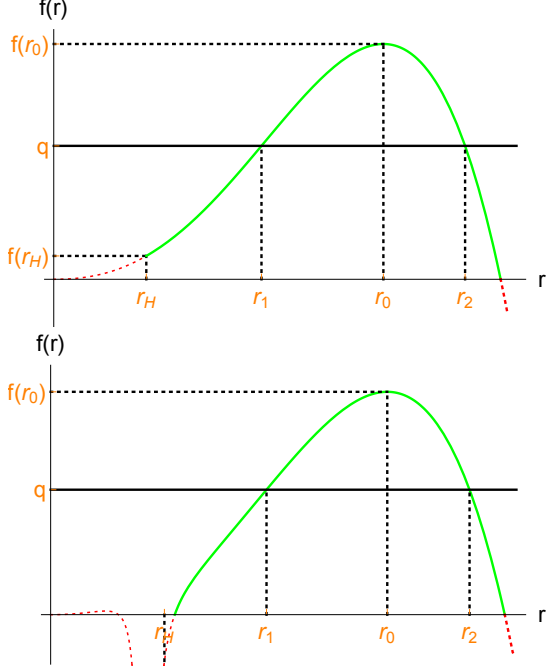


FIG. 2. Schematic diagrams of  $f(r)$ .  $r_1$  and  $r_2$  are shown to be roots of Eq. (28). Top:  $f(r)$  for extreme Kerr-Sen black hole. Bottom:  $f(r)$  for nonextreme Kerr-Sen black hole.

The extreme values of  $b_i$  ( $i = 1, 2$ ) are

$$\begin{aligned} b_i^s &\equiv b_i(r_i) \\ &= -\frac{a^2(c + r_i + 1) + r_i(2c^2 + c(3r_i - 2) + (r_i - 3)r_i)}{a(c + r_i - 1)}, \end{aligned} \quad (27)$$

where  $r_i$  is the solution of  $b'_i(r_i) = 0$  and  $r_1 < r_2$ .

We have the conditions that  $q \geq 0$  as well as  $r_* > r_H$ , but there still exist two possibilities, i.e.,  $r_* \leq r_1$  and  $r_* > r_1$ . To further confirm the relation between  $r_1$  and  $r_H$ , we need to analyze the equation

$$\begin{aligned} q &= f(r) \\ &= -\frac{r^2 \left( (2c^2 + c(3r - 2) + (r - 3)r)^2 - 4a^2(c + r) \right)}{a^2(c + r - 1)^2}, \end{aligned} \quad (28)$$

which is solved from  $b'_i(r) = 0$ . By calculation, we know that  $f(r)$  becomes maximum at  $r = r_0$  with

$$0 \leq r_0 = \frac{1}{2} \left( \sqrt{c^2 - 10c + 9} - 3c + 3 \right) \leq 3, \quad (29)$$

$$\begin{aligned} 4 &\leq f(r_0) \\ &= \frac{2 \left( \sqrt{c^2 - 10c + 9} - 3c + 3 \right)^2 \left( \sqrt{c^2 - 10c + 9} - b + 3 \right)}{\left( \sqrt{c^2 - 10c + 9} - c + 1 \right)^2} \\ &\leq 27, \end{aligned} \quad (30)$$

as well as

$$f(r_H) = 4a - a^2 > 0 \quad \text{for } a + c = 1, \quad (31)$$

$$\begin{aligned} f(r_H) &= \frac{(-c + \chi + 1)^2 (a^2 - 2(c^2 + c\chi + \chi + 1))}{a^2} \\ &< \frac{(-c + \chi + 1)^2 (a^2 - 2(c^2 + 1))}{a^2} \\ &< 0 \end{aligned} \quad \text{for } a + c < 1, \quad (32)$$

where  $\chi = \sqrt{(b - 1)^2 - a^2}$ . We show schematic diagrams for the two kinds of  $f(r)$  in Fig. 2. Different to the Kerr-Newman case in Ref. [1], we have  $q > 0$  at the event horizon for extreme Kerr-Sen black hole and  $q < 0$  at the event horizon for nonextreme Kerr-Sen black hole. As a result, we can know that there exist three cases about the relations of  $r_1$ ,  $r_H$  and  $r_*$ , which are

$$\text{Case (1): } r_1 < r_H < r_*, \quad (33a)$$

$$\text{Case (2): } r_H \leq r_1 < r_*, \quad (33b)$$

$$\text{Case (3): } r_H < r_* \leq r_1. \quad (33c)$$

We now determine the boundary of escape cone for a photon from the extreme or nonextreme Kerr-Sen black hole case by case. We will restrict the light source in the range  $r_H < r_* \leq r_0$  as the calculation is similar for  $r > r_0$ .

*Case (1)* This case appears only for extreme Kerr-Sen black hole as  $r_1 < r_H$ , which can be observed in the top diagram of Fig. 2. Combing the left diagram in Fig. 3 with the radial effective potential (7), we can know that there are two critical conditions that the photons just cannot escape to infinity. One is a radially inward photon with the impact parameter  $b = b_1(r_H)$  and the other is a radially outward photon with the impact parameter  $b = b_2^s$ . The radial momentum of the photon with the impact parameter  $b_2^s$  vanishes. So the critical angles that a photon can escape from the extreme Kerr-Sen black hole to infinity are

$$\begin{aligned} (\alpha_{(1)}, \beta_{(1)})_{\text{ext}} &= (\alpha, \beta) \Big|_{[\sigma_r = -1, b = b_1(r_H), 0 \leq q < f(r_H)]} \\ &\cup (\alpha, \beta) \Big|_{[\sigma_r = 1, b = b_2^s, 0 \leq q < f(r_H)]}, \end{aligned} \quad (34)$$

where  $b_1(r_H) = 2$ .

*Case (2)* As  $r_1 > r_H$ , we have  $f(r_H) \leq q < f(r_*)$  for extreme Kerr-Sen black hole and  $0 \leq q < f(r_*)$  for

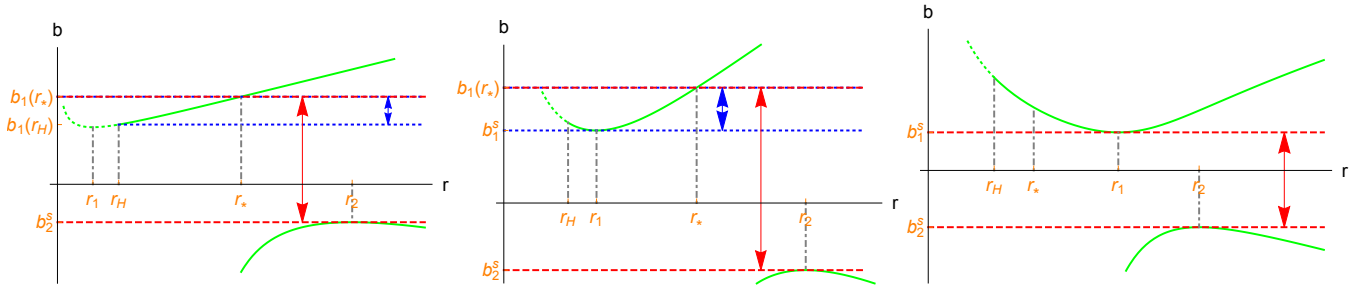


FIG. 3. The impact parameters  $b_i$  are shown for cases (1)-(3) in sequence. The photon with outward radial momentum can escape from the Kerr-Sen black hole in the range marked by the vertical red arrow. The photon with inward radial momentum can escape from the Kerr-Sen black hole in the range marked by the vertical blue arrow.

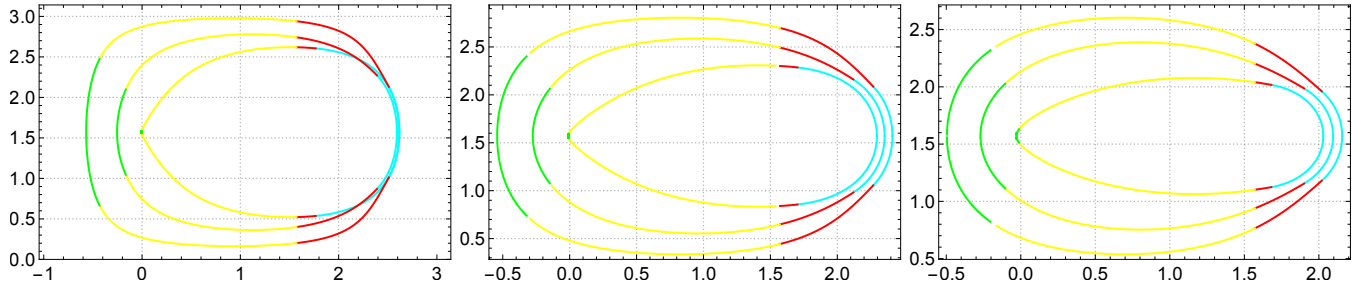


FIG. 4. Critical angles for extreme Kerr-Sen black hole. The vertical axes and horizontal axes stand for  $\beta_{(i)}$  and  $\alpha_{(i)}$ , respectively. Left:  $a = 1, r = 1.01, 1.5, 2$  from inside to outside. Middle:  $a = 0.5, r = 0.51, 0.75, 1$  from inside to outside. Right:  $a = 0.2, r = 0.21, 0.3, 0.4$ . The cyan, red and yellow curves individually stand for the former parts of  $(\alpha_{(i)}, \beta_{(i)})$  in Eqs. (34), (35) and (37), whose latter parts are represented by the green curves.

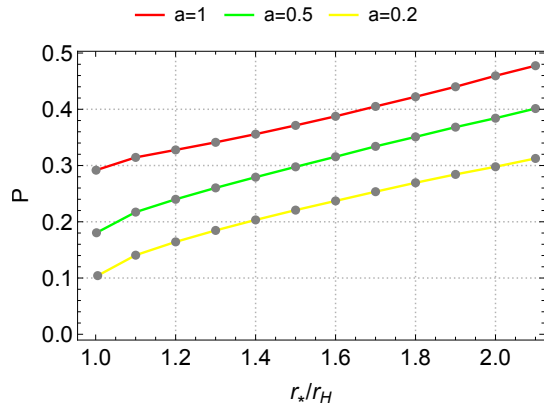


FIG. 5. Variations of the escape probabilities with respect to the radial position for the photons emitted from the extreme Kerr-Sen black hole.

nonextreme Kerr-Sen black hole. As shown in the middle diagram of Fig. 3, photons with impact parameters  $b_1^s$  and  $b_2^s$  can just move inward to a bounded circular orbit with radius  $r = r_1$  and move outward to the other bounded circular orbit with radius  $r = r_2$ , respectively. As a result, in this case, the critical angles that photons can escape from the extreme Kerr-Sen black hole to in-

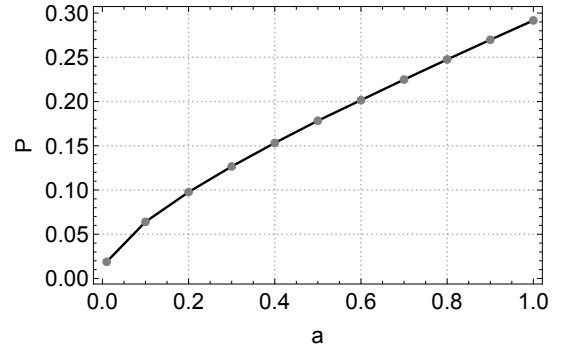


FIG. 6. Variations of the escape probabilities with respect to the angular momentum of the extreme Kerr-Sen black hole for the emitted photon in the horizon limit.

finity are

$$\begin{aligned} (\alpha_{(2)}, \beta_{(2)})_{\text{ext}} = & (\alpha, \beta)|_{[\sigma_r=-1, b=b_1^s, f(r_H) \leq q < f(r_*)]} \\ & \cup (\alpha, \beta)|_{[\sigma_r=1, b=b_2^s, f(r_H) \leq q < f(r_*)]}, \end{aligned} \quad (35)$$

and the critical angles that photons can escape from the nonextreme Kerr-Sen black hole to infinity are

$$\begin{aligned} (\alpha_{(2)}, \beta_{(2)})_{\text{n-ext}} = & (\alpha, \beta)|_{[\sigma_r=-1, b=b_1^s, 0 \leq q < f(r_*)]} \\ & \cup (\alpha, \beta)|_{[\sigma_r=1, b=b_2^s, 0 \leq q < f(r_*)]}. \end{aligned} \quad (36)$$

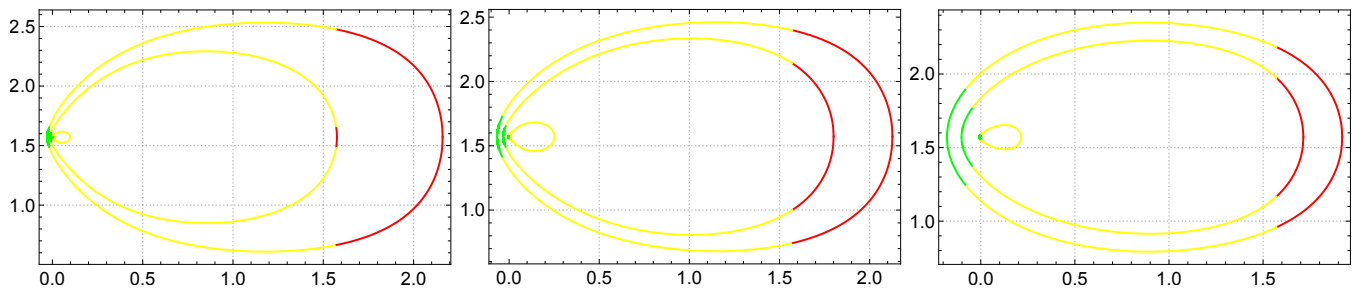


FIG. 7. Critical angles for non-extreme Kerr-Sen black hole with  $K = 0.999$ . The vertical axes and horizontal axes stand for  $\beta_{(i)}$  and  $\alpha_{(i)}$ , respectively. Left:  $a = 0.98$ ,  $r = 1.0253, 1.033, 1.06$  from inside to outside. Middle:  $a = 0.7$ ,  $r = 0.7386, 0.76, 0.8$  from inside to outside. Right:  $a = 0.3$ ,  $r = 0.3257, 0.36, 0.4$ . The red and yellow curves individually stand for the former parts of  $(\alpha_{(i)}, \beta_{(i)})$  in Eqs. (36) and (37), whose latter parts are represented by the green curves.

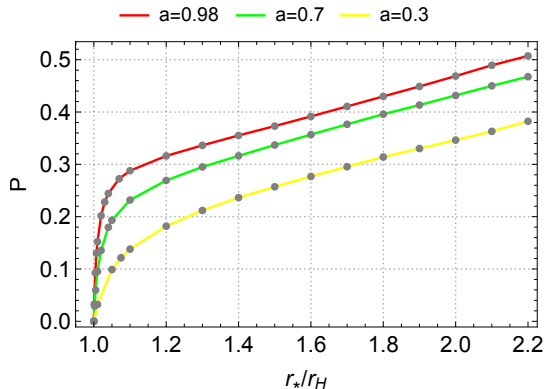


FIG. 8. Variations of the escape probabilities with respect to the radial position for the photons emitted from the nonextreme Kerr-Sen black hole with  $K = 0.999$ .

*Case (3)* There is not any radially inward photon that can escape from the Kerr-Sen black hole to infinity in this case. According to the right diagram in Fig. 3, the condition that the radially outward photons can go to infinity is  $b_1^s < b < b_2^s$ . Consequently, we get the critical angles of photons escaping from extreme or nonextreme Kerr-Sen black hole to infinity as

$$\begin{aligned} (\alpha_{(3)}, \beta_{(3)}) &= (\alpha, \beta)|_{[\sigma_r=1, b=b_1^s, f(r_*) \leq q < f(r_0)]} \\ &\cup (\alpha, \beta)|_{[\sigma_r=1, b=b_2^s, f(r_*) \leq q < f(r_0)]}. \end{aligned} \quad (37)$$

According to cases (a)-(c), we obtain the boundary of the escape cone for the photon escaping from the extreme or nonextreme Kerr-Sen black hole to infinity as

$$\partial S = \bigcup_{i=1,2,3} \left\{ (\alpha_{(i)}, \beta_{(i)})|_{\sigma_\theta=1}, (\alpha_{(i)}, \beta_{(i)})|_{\sigma_\theta=-1} \right\}. \quad (38)$$

The escape cone  $S$  is the solid angles surrounded by the critical angles. Note that the escape cone is symmetric to the equatorial plane of the Kerr-Sen black hole, which means  $\beta_{(i)}|_{\sigma_\theta=-1} = \pi - \beta_{(i)}|_{\sigma_\theta=1}$ .

Supposing that photons are emitted isotropically from the light source near the Kerr-Sen black hole, the escape

probability of the photons can be defined by

$$P(r_*) \equiv \frac{1}{4\pi} \int_S d\alpha d\beta \sin \beta. \quad (39)$$

In Ref. [1], the escape probability of photons emitted from a light source near the Kerr-Newman black hole was calculated using the coordinates  $r_i$ , as

$$P(r_*) \equiv \sum_{i=1}^2 \frac{(-1)^i}{2\pi} \int_{r_{c,i}}^{r_0} dr_i \frac{d\alpha}{dr_i} \cos \beta_i, \quad (40)$$

where  $r_{c,i}$  are solutions of  $f(r) = 0$ . We realize that the escape probability can be written in form of

$$P(r_*) \equiv -\frac{1}{4\pi} \int_S d\alpha d \cos \beta, \quad (41)$$

which means the probability is related to the warped escape cone  $\alpha - \cos \beta$  whose area can be calculated by numerical method.

Since the escape cones and escape probabilities of photons around extreme Kerr-Sen black hole are different from the nonextreme Kerr-Sen black hole case, we will now evaluate them separately.

### A. Extreme Kerr-Sen black hole

The horizon of the extreme Kerr-Sen black hole is  $r_h = a$ . The impact parameter reads

$$b_i^s = -\frac{r_i^2}{a} - a + 2r_i + 2, \quad (42)$$

where  $r_i$  can be obtained from

$$q = f(r_i) = -\frac{r_i^2 (4a^2 - 4a(r_i + 1) + r_i^2)}{a^2}. \quad (43)$$

We show critical angles for photons emitted from a light source near the extreme Kerr-Sen black hole in Fig. 4. We can see that even if the position of the light source approaches the horizon, the escape cone of the photon does

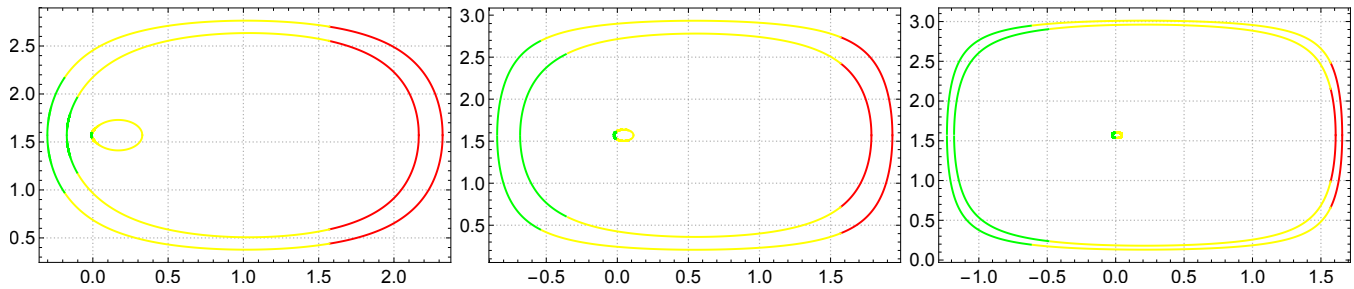


FIG. 9. Critical angles for non-extreme Kerr-Sen black hole with  $K = a$ . The vertical axes and horizontal axes stand for  $\beta_{(i)}$  and  $\alpha_{(i)}$ , respectively. Left:  $a = 0.98$ ,  $r = 1.2, 1.4, 1.6$  from inside to outside. Middle:  $a = 0.7$ ,  $r = 1.715, 2.2, 2.4$  from inside to outside. Right:  $a = 0.3$ ,  $r = 1.9543, 2.68, 2.75$ . The red and yellow curves individually stand for the former parts of  $(\alpha_{(i)}, \beta_{(i)})$  in Eqs. (36) and (37), whose latter parts are represented by the green curves.

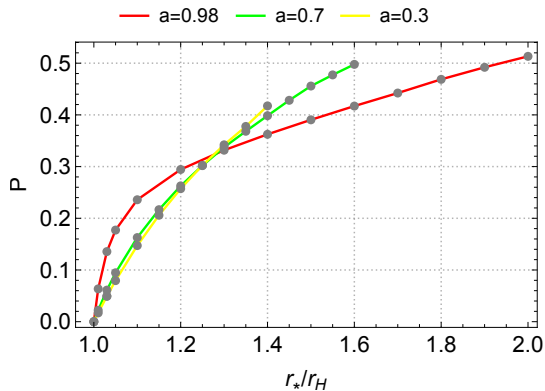


FIG. 10. Escape probability of the photon emitted from the nonextreme Kerr-Sen black hole with  $K = a$ .

not vanish. We further evaluate the escape probabilities of the photons at different positions around extreme Kerr-Sen black hole with different angular momentum in Fig. 5. We know that the escape probability of the photon increases with radial distance relative to the horizon. As seen in Fig. 6, the escape probability of the photon in the horizon limit increases with the angular momentum  $a$  of the extreme Kerr-Sen black hole. Note that  $P \rightarrow 0$  for  $a \rightarrow 0$ , and  $P \sim 0.292$  for  $a = 1$  (which is the extreme Kerr black hole case that has been discussed in Ref. [1]).

### B. Nonextreme Kerr-Sen black hole

We set  $c = K - a$  with  $0 < K < 1$  for the nonextreme Kerr-Sen black hole. In Fig. 7 and Fig. 8, we show the escape cones and the escape probabilities of the photons near the horizon of the nonextreme Kerr-Sen black hole with  $K = 0.999$ . We can see that the escape cones shrink and the escape probabilities decrease with the decreasing of the radial distance relative to the horizon of the nonextreme Kerr-Sen black hole. Especially, when the light source approaches to the horizon, the escape cones become vanishing and the escape probabilities become

zero. When we set  $c = 0$  for the nonextreme Kerr-Sen black hole, we can see similar results as shown in Figs. 9 and 10.

## IV. CLOSING REMARKS

The observations of the black hole shadow, high-energy physics and electromagnetic spectrum accompanied by gravitational waves from the black hole merger to some extent rely on the escape probabilities of the particles from the black hole. We investigated the escape probability of the photons from the Kerr-Sen black hole, inspired by the work in Ref. [1] where the escape probabilities of the photons in the Kerr-Newman spacetime were explored.

The light source was set to be at rest in a locally nonrotating frame on the equatorial plane of the Kerr-Sen black hole. After defining the emission angles, we calculated the escape cones and escape probabilities of the isotropically emitted photons both from extreme and nonextreme Kerr-Sen black holes. As a result, we found that, under the extreme Kerr-Sen black hole background, the escape cones are nonvanishing and the escape probabilities are nonzero in the event horizon limit; under the nonextreme Kerr-Sen black hole background, the escape cones shrink to be null and the escape probabilities become zero in the event horizon limit. Our result makes it clear that near horizon physics of the extreme Kerr-Sen black hole is more visible than that of the non-extreme Kerr-Sen black hole.

Our result is different from the one in Ref. [1] which shows that not all extreme Kerr-Newman black holes share nonzero photon escape probabilities in the horizon limit. We evaluated the escape probabilities of photons directly by calculating the area of the warped escape cones, which is also different from the way used in Ref. [1] where intermediate variables  $r_1$  and  $r_2$  where the impact parameters get extreme values were used. Nevertheless, we find a common property for the escaping probability, that is, if the emissions do not vanish in the horizon limit, the escape probabilities increase with the angular

momentum of both kinds of black holes.

It will be instructive to investigate the photons emitted from a light source moving on the circular orbit [23] and other kinds of sources [24, 25] in the Kerr-Sen black hole background. It is also meaningful to study the escape probability of the photon from a source off the equatorial plane based on the discussion of the photon emissions in Ref. [26]. We will leave them as future work.

## ACKNOWLEDGEMENTS

Jie Jiang is supported by the National Natural Science Foundation of China (Grants No. 11775022 and 11873044). Ming Zhang is supported by the Initial Research Foundation of Jiangxi Normal University with Grant No. 12020023.

- 
- [1] K. Ogasawara, T. Igata, T. Harada, and U. Miyamoto, *Phys. Rev. D* **101**, 044023 (2020), [arXiv:1910.01528 \[gr-qc\]](#).
  - [2] K. Ogasawara, T. Harada, U. Miyamoto, T. Igata, and M. Patil, *Phys. Rev. D* **95**, 124019 (2017), [arXiv:1609.03022 \[gr-qc\]](#).
  - [3] K. Akiyama et al. (Event Horizon Telescope), *Astrophys. J.* **875**, L1 (2019).
  - [4] K. Akiyama et al. (Event Horizon Telescope), *Astrophys. J.* **875**, L2 (2019).
  - [5] K. Akiyama et al. (Event Horizon Telescope), *Astrophys. J.* **875**, L3 (2019).
  - [6] K. Akiyama et al. (Event Horizon Telescope), *Astrophys. J.* **875**, L4 (2019).
  - [7] K. Akiyama et al. (Event Horizon Telescope), *Astrophys. J.* **875**, L5 (2019).
  - [8] K. Akiyama et al. (Event Horizon Telescope), *Astrophys. J.* **875**, L6 (2019).
  - [9] T. Igata, H. Ishihara, and Y. Yasunishi, *Phys. Rev. D* **100**, 044058 (2019), [arXiv:1904.00271 \[gr-qc\]](#).
  - [10] R. Penrose and R. Floyd, *Nature* **229**, 177 (1971).
  - [11] J. D. Schnittman, *Phys. Rev. Lett.* **113**, 261102 (2014), [arXiv:1410.6446 \[astro-ph.HE\]](#).
  - [12] O. Zaslavskii, *Phys. Rev. D* **93**, 024056 (2016), [arXiv:1511.07501 \[gr-qc\]](#).
  - [13] K.-I. Maeda, K. Okabayashi, and H. Okawa, *Phys. Rev. D* **98**, 064027 (2018), [arXiv:1804.07264 \[gr-qc\]](#).
  - [14] M. Zhang, J. Jiang, Y. Liu, and W.-B. Liu, *Phys. Rev. D* **98**, 044006 (2018).
  - [15] Y. Liu and W.-B. Liu, *Phys. Rev. D* **97**, 064024 (2018).
  - [16] Y. Liu and X. Zhang, *Eur. Phys. J. C* **80**, 31 (2020), [arXiv:1910.01872 \[gr-qc\]](#).
  - [17] B. Abbott et al., *Astrophys. J.* **848**, L12 (2017), [arXiv:1710.05833 \[astro-ph.HE\]](#).
  - [18] B. Abbott et al. (LIGO Scientific, Virgo), *Phys. Rev. Lett.* **116**, 061102 (2016), [arXiv:1602.03837 \[gr-qc\]](#).
  - [19] M. Zhang and J. Jiang, (2020), [arXiv:2004.03367 \[gr-qc\]](#).
  - [20] A. Sen, *Phys. Rev. Lett.* **69**, 1006 (1992), [arXiv:hep-th/9204046](#).
  - [21] B. Carter, *Phys. Rev.* **174**, 1559 (1968).
  - [22] J. M. Bardeen, W. H. Press, and S. A. Teukolsky, *Astrophys. J.* **178**, 347 (1972).
  - [23] T. Igata, K. Nakashi, and K. Ogasawara, *Phys. Rev. D* **101**, 044044 (2020), [arXiv:1910.12682 \[astro-ph.HE\]](#).
  - [24] O. Semerák, *Helvetica Physica Acta* **69**, 69 (1996).
  - [25] Z. Chang and Q.-H. Zhu, *Phys. Rev. D* **101**, 084029 (2020), [arXiv:2001.05175 \[gr-qc\]](#).
  - [26] D. Gal'tsov and K. Kobialko, *Phys. Rev. D* **99**, 084043 (2019), [arXiv:1901.02785 \[gr-qc\]](#).